



## **Implementation of Closing Eyes Detection with Ear Sensor of Muse EEG Headband using Support Vector Machine Learning**

Erwin Sutanto<sup>1\*</sup>Teguh Wijaya Purwanto<sup>2</sup>  
Weryyan Shalannanda<sup>5</sup>Fahmi Fahmi<sup>3</sup>  
Muhammad Aziz<sup>6</sup>Muhammad Yazid<sup>4</sup>

<sup>1</sup>*Biomedical Engineering, Faculty of Science and Technology, Universitas Airlangga, Kampus C Mulyorejo, Surabaya 60115, Indonesia*

<sup>2</sup>*PT. Teknologi Otak Kekinian, Surabaya, Indonesia*

<sup>3</sup>*Department of Electrical Engineering, Universitas Sumatera Utara, Medan, Indonesia*

<sup>4</sup>*Biomedical Engineering Department, Institut Teknologi Sepuluh November, Indonesia*

<sup>5</sup>*School of Electrical Engineering and Informatics, Bandung Institute of Technology, Bandung, Indonesia*

<sup>6</sup>*Institute of Industrial Science, The University of Tokyo, Japan*

\* Corresponding author's Email: [erwin\\_sutanto@fst.unair.ac.id](mailto:erwin_sutanto@fst.unair.ac.id)

**Abstract:** Epilepsy patients might need continuous electroencephalography (EEG) monitoring to help them understand their own condition's improvements or their doctors to determine the frequency of the seizures. In this study, we demonstrated how a low-cost, portable EEG headband could be used to detect absence seizures in epilepsy patients. The method used is Support Vector Machine (SVM) to separate the initial limit and Machine Learning with Tensorflow to predict its confidence level. Then, we tried to test our method on 2 other patients to see its measurement divergence. Furthermore, the Tensorflow library has been applied and developed to train and classify the data, which is also one of the novelty approaches in this study. From the result, closed eyes can be detected from open-eye conditions with more than 96 % accuracy and a loss of only 2.35%. The findings demonstrate the feasibility of detecting absence seizures using only two electrodes which were TP9 and TP10 of Muse headband which is also positioned in the ear like an ear-EEG. Overall, the study successfully developed a novel method utilizing a low-cost headband to provide affordable health system access.

**Keywords:** Muse headband, Node js, Epilepsy, Health system access, Rapid detection, Good health, Well-being.

### **1. Introduction**

Epilepsy occurs due to irregular brain activity (seizure). The seizure itself activates neurons in the brain that occurs synchronously. This irregularity problem can occur because of a chemical reaction in the brain that results in activation that does not work or it could be due to inhibition that does not occur. The network chemistry processes that work irregularly can result in multiscale periodicities [1]. Disruption of this process can occur due to tumors [2], infection [3], or injuries related to the brain. In fact, it can also cause other psychological effects such as depression, suicide, injuries, and mortality. Thus, the

rapid detection of the seizure would help the individual as a well-being.

Easy diagnosis is very helpful for patients with epilepsy. The commonly used diagnosis for this disease is by using an electroencephalography (EEG) signal which is suggested in [4]. With EEG, biopotential signals from the brain can be obtained from the surface of the patient's head. In general, this EEG signal analysis is conducted in the hospital using many signal lines (channels) and will interfere with patient activities. The total number of commonly used channels is 20 from the international standard of 10–20 system electrodes [5]. Long observations to obtain sufficient and comprehensive data from each part of the brain are often one of the obstacles [6].

This is necessary because brain surgery itself is not simple and needs to be done with great precision [7]. Therefore, doctors or medical experts who treat patients need to be assisted with an EEG tool to make an accurate diagnosis. It can also be combined with IoT (Internet of Things) [8].

Epilepsy seizures themselves can be seen from the outside in the form of patient movements such as muscle stiffness, jerking, and loss of response. In addition, it can also be easily detected from eye movement-related activities [9]. However, because they are unconscious, patients often do not know what happens when the seizure occurs. In order to be able to make an early and frequent diagnosis, patients also need to know more about their epilepsy. To detect epilepsy rapidly, we need to know its common signs. The simplest symptom of loss of consciousness can be seen from a blank stare [10].

Although advances in research on quantitative EEG prediction metrics have been made, in general, rapid detection research uses only available EEG datasets and does not apply directly to patients, such as by using the university of Bonn epilepsy EEG dataset [11]. Challenges still preclude the routine clinical use of the EEG as a monitoring or diagnostic tool. Typically, setting up and recording conventional EEG devices can be time-consuming, with many of the setups in previous investigations using nineteen or more electrodes [12]. Many of these issues can be solved by using a portable EEG that can be owned by every patient as each patient has their own characteristic [13]. This rapid detection would detect possible epilepsy from the signal recorded using a portable EEG device. EEG recording systems costing less than 500 USD that we can classify as low-cost EEG devices, have been widely circulated in recent years [14]. One of the affordable EEG headbands is Muse™ product which could also be used for states of calmness and alertness [15].

EEG can be seen as a superior modality for detecting brain signal given recent developments and the commercial availability of this low priced EEG headsets [16]. This affordable and portable technology can be easily integrated into everyday monitoring and better triage to help when seizures occur if the data obtained using the Muse has sufficient sensitivity to differentiate epilepsy patients from controls (e.g., blank stare). The most typical sign of an epilepsy patient is absence seizures. It is classified as generalized seizures [17]. However, only a small number of studies have been conducted to confirm its usefulness in the study of epilepsy-related brain potential. Despite the fact that MUSE™ also has a software development community that

allows scientists to access raw data for research purposes.

Several studies point to wearable EEG recording devices called ear-EEGs. These devices depend on recording electrodes as earpieces specially designed to fit the external ear canal. The idea has been tried for seizure detection in epileptic patients and for sleep recordings in healthy individuals [18]. An ear-EEG placed behind the ear during a seizure was also found to have a temporal waveform and frequency content similar to that of a scalp EEG [19]. What's interesting here is that the Muse headband also has a conductive electrode which we can classify as ear-EEG because it is also in the position on the ear.

Here, we hypothesized that the trade-off between electrode location and ease of use would be beneficial for detecting basic eye activity and would also be detectable with the Muse headband where its use is much more efficient at a fraction of the cost. In this experiment, we would utilize the developer community with its open-source development library muse-js to access the headband. From the software, the headband's parameters, such as the remaining battery charge, three axis accelerometers, and its 5 EEG electrodes could be accessed by using the most used chrome web browser through its extension.

The main aim of this study was to investigate how to identify closed eyes from open eyes condition so as to demonstrate suspected absence seizures (i.e., "blank stare") using inexpensive portable EEG equipment. This typical seizure is easily indicated from a few seconds from the open eyes condition (without closed eyes) by patients. In other words, without the detection of closed eyes within a few seconds, these can be referred to as absence seizures [20] or petit mal seizures [17]. By understanding that, we can start diagnosing with these signs.

We also explore the confidence level to detect the difference between closed and open eyes using machine learning. From this process the accuracy and loss values of the learning model will be obtained. Lastly, measurement divergence is also tested by applying the method to two other subjects.

The organization of this paper is as follows: in section 2, we outline the methodology we used in this investigation; in section 3, we present the findings with the use of a Muse headband; and in section 4, we make comparisons with results from other studies which using same headband. Finally, the conclusion is in section 5.

## 2. Methods

In this section, we will describe the experiments carried out to detect the condition of closed eyes in

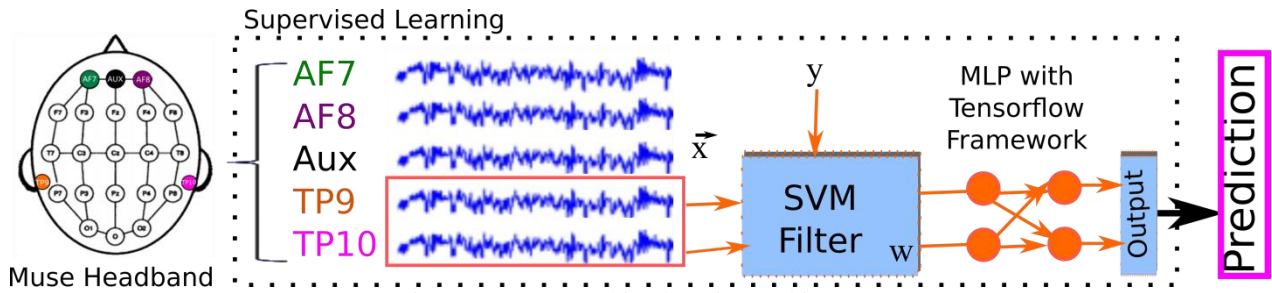


Figure. 1 SVM machine learning architecture

which two methods will be used. The first is the support vector machine (SVM) to get the level of separation automatically. Then, multi layer perceptron (MLP) will be used in training to study eye activity detection. Finally, before we could further analyze the wearable headbands use, we will also discuss the possibility of detecting epilepsy using eye activity.

### 2.1 Support vector machine

In this research we try to distinguish the closed eye signal from the open eye signal with the Support Vector Machine (SVM) as in ear-EEG application at [19]. The entire experimental setup can be seen Fig. 1.

$$x \in \mathbb{R}^D \quad (1)$$

$$\phi: \mathbb{R}^D \rightarrow \mathbb{R}^M, \phi(x) \in \mathbb{R}^D \quad (2)$$

Once the EEG data has been successfully collected symbolizes by  $x$ , the clustering method is carried out by mapping the  $x$  data to the  $\mathbb{R}^D$  coordinate system. The classification of training conditions is carried out by  $\phi(x)$  and in the data it can be indicated from the condition of the eyes being closed or open. The simplest separation will be written in a dividing line known as the Support Vector Machine (SVM).

$$\mathcal{H}: w^T \phi(x) + b = 0 \quad (3)$$

The above equation will be the decision boundary of the data to be processed. The  $w^T$  matrix is the load to decide whether the eye is in an open or closed condition. Also,  $b$  is the bias value of the above linear equation. Where the value of  $d_H$  is the value of the distance in general as in Eq. (4).

$$d_H(\phi(x)) = \frac{w^T \phi(x) + b}{\|w\|^2} \quad (4)$$

It is likely that the value will correspond to Eq. (3). Whether the value will be less than zero ( $d_H < 0$ ) or greater than zero ( $d_H > 0$ ) or equal to zero ( $d_H = 0$ )

when the equation is on the line, each will determine which cluster will be followed by the point. The perfect separation condition, with decidedly level  $L$ , can be obtained by finding its value by determining the loading  $w^*$  which follows this condition:

$$w^* = \underset{w}{\operatorname{argmax}} [\min_n (d_H(\phi(x_n)))] \quad (5)$$

To find the solution, Eq. (4) can be substituted for Eq. (5). However, this solution can only be used for ideal conditions where there is no intersection between the two clusters.

$$w^* = \underset{w}{\operatorname{argmax}} [\min_n \frac{y_n [w^T \phi(x_n) + b]}{\|w\|^2}] \quad (6)$$

The value of  $y_n$  is the output of Eq. (3). Optimization can be done by processing the above data by simplifying it into Eq. (7).

$$w^* = \underset{w}{\operatorname{argmax}} \frac{1}{\|w\|^2} \quad (7)$$

$$s. t. : \min_n (y_n [w^T \phi(x_n) + b]) = 1 \quad (8)$$

In real conditions, there is often a wedge between the two clusters, so it is necessary to add an error value of  $\zeta$ .

$$w^* \rightarrow \min_{w, b, (\xi_n)} \frac{1}{2} \|w\|^2 + C \sum^n \xi_n \quad (9)$$

$$s. t. : \min_n (y_n [w^T \phi(x_n) + b]) \geq 1 - \xi_n \forall n, \xi_n \geq 0 \forall n \quad (10)$$

This optimization is described into Algorithm 1. This algorithm shows the order of our experiment. It started with acquiring data for two conditions, open and closed eyes.

The data obtained is then divided so that it can be used for training and testing. Furthermore, the model that has been made will be trained to recognize the pattern of the two conditions. Finally, testing is

---

Algorithm: 1 EEG support vector machine of this study

---

**Input:** EEG vector  $X = [x_1, x_2, \dots, x_n]$ .  
 Label data set  $Y = [y_1, y_2, \dots, y_n]^T$ .  
**Output:** The optimized value  $w^*$ , and Separation Level L.  
**Require:** node.js, muse.js, jquery, and popper.js  
 1: Install Muse headband to Subject Head and run Mindjam  
 2: Collecting Data from Subject with Open Eyes  
 3: Collecting Data from Subject with Closed Eyes  
 4: Split Data for Training and Testing  
 5: Initialize  $\phi(x)$  and b  
 6: **while** not convergence **do**  
 7:     Calculate  $w^* \rightarrow \frac{1}{2} \|w\|^2$   
 8:     **if success then**  
 9:         Calculate Separation Level L  
 10:         Exit  
 11:     **else**  
 12:          $n = n + 1$   
 13:     **end if**  
 14: **end while**  
 15: Run Machine Learning Training

---

carried out. From the test results, it will be determined whether the introduction of the two conditions is good enough or not. If the result is not good, then it will be remodeled and retested. When it is finished, the model remains to be used by patients. If possible, there will be subdivisions among wide-awake values and closed eyes for the same values. It could also make an ideal range transfer. Uncertainty at the boundary will be seen in the transition chart. This might happen when the conscious mind is dicey in the real application.

## 2.2 Multi layer perceptron

Multi layer perceptron (MLP) would be possible with the intake of EEG signal as an input variable. The machine learning method could be used to learn which later will be useful for us to justify its output classification. In this case, eye movements would be classified. The closed eye would be classified by 0, while a wide-awake condition is represented by 1. The seizure prediction from EEG signal had been evaluated from the mean difference as shown in Eq. (11) as described in [21].

$$MAD(x) = \frac{1}{N} \sum_{i=0}^{N-1} |x(i) - \bar{x}| \quad (11)$$

N is the number of data points in the signal sequence x. x(i) is the signal value x in the i-th order.

Meanwhile,  $\bar{x}$  is the average value. Moreover, it is important to choose the best Artificial Neural Network (ANN) model in order to find the differences between those two conditions. Methods from ANN have to be tested and verified with its accuracy and loss rate. Because our application is a kind of recognition pattern, the best function would have high accuracy and a low loss rate.

To realize, the function of the activation of the machine, we could use any functions, either the sigmoid or tanh function. Both could permit in a similar way but has different transitions.

$$f(x) = \frac{1}{1+e^{-x}} \quad (12)$$

The Sigmoid at Eq. (12) is working at a positive input range. Meanwhile tanh function could have values from negative values. It might be with x as input of EEG signal, and f(x) as the classification of eye conditions. The data set would be using Muse EEG data. This might be achieved by recording the eye movement for about one minute. A convergence value can be achieved if the data could be classified. It would then be used to get patterns for each classification. Conversely, if the data is difficult to be classified, it will make the machine learning have an over-fitting situation to study the difference. Preparation of the validation dataset would be directly partitioned from training data. This builds the weighing factors in a straight forward process. A model of ANN and the chosen method would have the prediction of the data as in [22]. In making independent and dependent factors from the dataset, we should spare the data for testing. Using ANN, we could use three types of layers. The layers are input, hidden, and output. Using these layers, we could include the machine learning methods to have different activation functions.

$$f(x) = K(\sum_i \omega_i g_i(x)) \quad (13)$$

The first layer is the layer that has our input. Not many calculations occur at this part. This is used to condition the data before going into the hidden layer. The hidden layer is the layer separating input from the output. It could have many layers. These layers would have extensive calculations before sending the data to the output side. Finally, the output is the last layer of the network that will decide the classification. With proper training, machine learning could give the best classification for our EEG Signals.

TensorFlow could be useful as an interface to try machine learning methods. Tensors themselves are actually relevant to vectors and their following spaces.

It might have different factors, such as scalar, vector, vectors at one point, or a map between vectors [23]. This might be suitable for our application in this experiment as long as it can be a kind of tensor [24].

$$T = [T^{(e1)} \quad T^{(e2)} \quad T^{(e3)}] = \begin{bmatrix} \sigma_{11} & \sigma_{12} & \sigma_{13} \\ \sigma_{21} & \sigma_{22} & \sigma_{23} \\ \sigma_{31} & \sigma_{32} & \sigma_{33} \end{bmatrix} \quad (14)$$

T represents a vector of stresses as an act from the center of a cube which correspondence with the orthogonal planes of e1, e2, and e3. Tensor T is built from other vectors. A working system would be able to identify the eye movement at the testing stage. In this study, testing of the eye movement dataset would be done using the accuracy and loss rate of the predictions. Along with the training and validation, the accuracy and loss rate of our machine learning model will be summarized. It would show the probability of eye’s movement into open or close state. For the application, we could just use Keras Library. It provides many activation functions to model our machine learning. Once it is built and fitted, the model could be validated. The validation can be used to identify whether the system can classify our dataset. In comparison with [11], which was combined using local binary pattern with binary values of 0 and 1 value only, this method has a prediction value with a decimal score from 0 to 1 represented as confidence level and one with 100% confidence.

### 2.3 Muse™ Headband

Absences can be classified as generalized non-motor seizures in the new ILAE classification [25]. Table 1 shows most epilepsy types related to eye activity [17]. The consciousness of the eye’s movement might also be related to static representations of the brain’s physical cognitive state or representation of its statistical connectivity as described in persistent networks in its long-term intracranial [26]. However, the long period of brain connectivity which exists from transient activity emerges less likely to happen [17]. By having its signals recorded, we would be able to see if the Muse headband has the capability to detect it.

The standard for EEG electrode notation is the international 10-20 system. It has divided into brain parts. First is the brain hemisphere of the left and right brain. It differentiates each other with the number following the letter. The right brain is followed by even numbers while the left one is by odd

Table 1. The classification of typical absence seizures

No.	Name	Description	Ref.
1	Centrecephalic Epilepsy	Petit Mal or Typical Absence Seizure	[27], [28]
2	Idiopathic Epilepsy	Absence Epilepsy which happened during childhood, and juvenile absence	[29]
3	Other generalized onset nonmotor seizures	Typical nonmotor absence seizures, and differentiated	[25]
4	Dialeptic Seizures	A typical ictal EEG, and complex partial seizures as dialeptic seizures together with a focal ictal EEG	[30]

numbers. There is also a letter to code each area of the brain. They are AF, F, T, TP, C, P, and O for anterior frontal, frontal, temporal, temporal-posterior, central, parietal, and occipital consecutively.

Muse™ headband is incorporated with five electrodes. They are Aux, AF7, AF8, TP9, and TP10 following the electrode position nomenclature [31]. Aux, AF7, AF8 are on the forehead as shown in Fig. 1 with black, green, and purple colors respectively, and works like a scalp EEG. However, TP9 and TP10 are in the left and right ears respectively as shown in Fig. 1 with orange and pink respectively. These last two sensors work in a different way unlike the previous three electrodes with the scalp EEG type. Both were kind of smart sensor which was introduced commercially as “smart sense conductive rubber ear sensors.” It should already have an intelligence sensing mechanism. Meaning that as long as the sensor touched the ear surface, data would still be obtained as the similar mechanism worked in ear-EEG Sensors [32]. This can be compared to the ear-EEG sensor in [19] which is behind the patient’s ear. In [19], there are four electrodes divided into two on each left and right ear. Both groups of sensors work with a potential difference between the electrodes.

Since it has only five compared to the standard 10-20 System, which has more than 15 channels, it has a limitation on detecting our EEG, for example, it might be used to predict stroke severity but only for rapid diagnosis [33]. It also has an accelerometer and gyroscope to ensure that the detection is based on the EEG signal and not from the headband movement. The structure of this band gains an advantage of its portability. It can be easily released and used as a normal head band.

Table 2. Code description

No.	Data	Description
1	Current code version	v1.0
2	Permanent link to code/repository used for this code version	<a href="https://github.com/jaycode/mindjam">https://github.com/jaycode/mindjam</a>
3	Legal Code License	MIT
4	Software code languages, tools, and services used	javascript
5	Compilation requirements, operating environments & dependencies	node-js, muse-js, jquery, and popper.js

One application using Muse headband could detect head movement [34]. However, it does not have eye movement detection. There is a suggestion of using an alpha frequency signal to detect the movement [35]. However, this rapid detection uses simple detection for comparison with another simple method [11]. It would be first verified with its statistical value such as its average value and standard deviation to see the possibility. Then, the machine learning approach would qualify it using neural cells to learn from its mean absolute deviation (MAD) values.

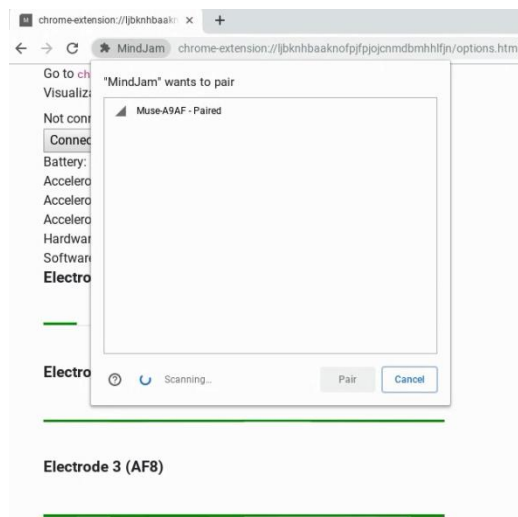
### 3. Result and discussion

The software was running in Google Chrome browser using its extension app development features. It was also using Android operating system for the test. By using this software, we could see raw data of EEG signals from our Muse headband.

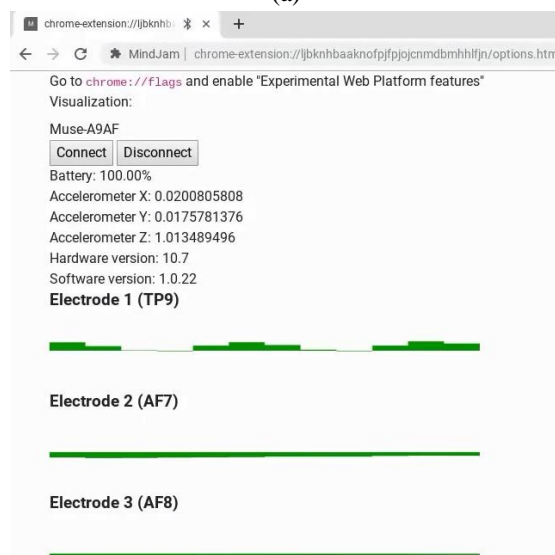
#### 3.1 Software architecture

MindJam was written in node JS and used the following libraries to access Muse headband via Bluetooth:

Mindjam used the main library of muse-js [36] which is built on node JS to access Muse using Web Bluetooth. From the muse-js, we brought it to the chrome architecture by using its extension interface. We had also changed the display for the EEG channel and the accelerometer axis from that main library. The generated data from mindjam was electrode's voltage raw value in uV ( $10^{-6}$  Volt). Using this software, we could look into the EEG signals gathered by the Muse headband. Another library was jquery [37] for javascript query access. Finally, popper.js [38] was used for the tool-tip and popup positioning feature.



(a)



(b)

Figure. 2 Accessing Data with Chrome Extension: (a) Connect to MuseTM Headband and (b) Reading EEG Electrodes.

#### 3.2 Software functionalities

There were two major functionalities of this software. The first one was to connect with the Muse headband in Fig. 2 (a). The second usage was to display the data read by the Muse headband in Fig. 2 (b). These two screens showed how we accessed the headband at our App.

Once the Headband is switched on, we would see the Muse device in the list as shown in Fig. 2 (a). Then, the pairing process would be started through this App. Since we used Muse 2 headband, we did not need to pair our device through Bluetooth manually. After that, we just waited for the device to be connected to our chrome book through Bluetooth.

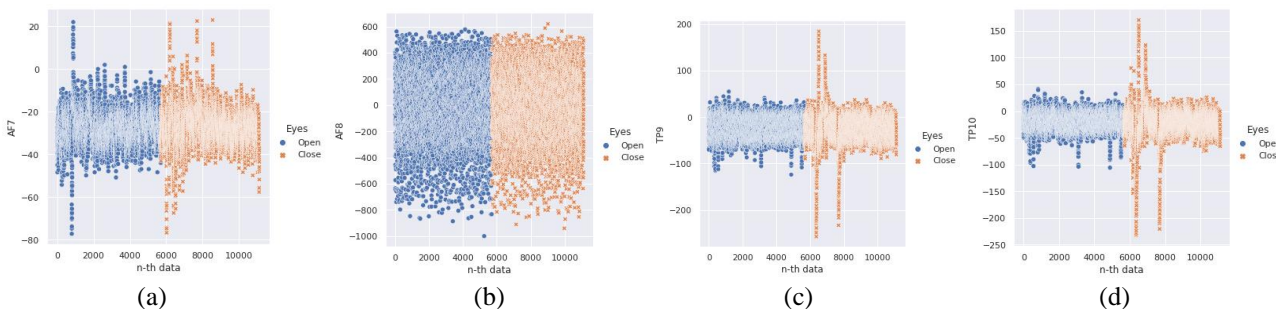


Figure. 3 Recording dataset from wearable headband. The blue color was for open eyes and the red color for close eyes: (a) AF7, (b) AF8, (b) TP9 and (d) TP10

Table 3. The EEG data statistics

Condition	TP9 (uV)		TP10 (uV)		AF7 (uV)		AF8 (uV)		AUX (uV)	
	Open	Closed	Open	Closed	Open	Closed	Open	Closed	Open	Closed
count	5712	5412	5712	5412	5712	5412	5712	5412	5712	5412
mean	-22.73	-25.54	-19.7	-23.03	-27.05	-26.73	-29.16	-27.81	19.84	13.12
std	24.25	36.09	16.99	32.54	8.38	9.06	271.9	269.87	131.01	129.49
min	-124.02	-257.32	-105.96	-232.91	-77.15	-76.66	-1000	-940.43	-295.9	-295.9
25%	-41.99	-43.95	-32.23	-35.16	-32.23	-32.23	-218.75	-215.45	-72.75	-79.1
50%	-22.46	-23.93	-19.53	-21.73	-27.34	-26.86	-25.88	-19.53	-2.44	-11.47
75%	-2.93	-4.39	-7.32	-7.81	-21.97	-21.97	184.57	177.86	83.5	76.66
max	54.69	184.08	41.5	170.41	21.97	22.95	577.64	620.12	571.78	563.96

Next, we would see the interfaces filled with data from our headband, as shown in Fig. 2 (b).

The obtained data from the headband were the battery remaining charge, the accelerometer’s data with its three axis; X, Y, and Z, then, and the electrode’s data which were TP9, AF7, AF8, TP10, and AUX as shown respectively. All those presented data were the available data for being utilized. For example, the axis could be used for head movements. Then, the battery’s remaining capacity could help us prepare for any emergency or power shortage. Meanwhile, electrode’s data was the one that could help us investigate our brain signals.

The signal itself was biopotentials. This was not strong enough and prone to noise. This made most of the applications use filters to reduce the noise. In terms of noise, some indications showed that the headband movement would affect the signals. This was a disadvantage most of all surface-based electrodes where the shift of electrodes on the scalp would cause noise or interference with the signal from the EEG. The other characteristic of the signals was their small values. They were only in micro Volts ranges. Thus, it is also required to be amplified before being used. Under all of these conditions, we had been helped with this commercial Muse headband. It had been packaged with this kind of required signal processing and its communication interface. It also

had its developers community to utilize the headband for any research especially using node js [36].

The Muse headband gave us the possibility to take care of only the signal analysis to achieve our goal. In this case, it was about catching epilepsy signs. As suggested before a typical seizure, could be staring activities or unblinking eyes for a long period, as listed before in Table 1. Itemizing those activities would bring us into the basic two activities which were open and close. As we could see from the interface in Fig. 2 (b), the data would be changed based on the EEG headband sensor’s data; we could just test the recording data with the basic two movements. From the EEG recoding data, we would be able to classify how far the headband could be utilized for detecting those movements.

Table 3 shows us the statistics from both conditions open and close. The values were showed us more details about the differences. The gap values between each channel could be more quantified than just visible from the figure before. By calculating the gap for each TP9 and TP10 from Table 3, there would be 178.71, 441.41, and 147.46, 403.32uV for each open and close at channel TP9 and TP10 respectively. There was more than 250 uV for each channel. This number was promising enough for the detection of our basic movements. For comparison, channel AF7 and AF8 have much lower values. The gaps for each

channel AF7 and AF8 were only 0.49 and -17.09 $\mu$ V. Thus, we could just decide to use TP9 and TP10 for the detection. Other methods would try to get value by using the ref value of AUX. It would also be possible as the mean value of AUX is only at 19.84 $\mu$ V and 13.12  $\mu$ V for each open and close of eyes condition in order. Similarly as described before with MAD value [21], we could just try to use the individual value with the compensation of machine learning. Using machine learning, there was a possibility to use more than one signal [39]. It will simplify our model into just one model for overall signals. It was better than two individual model for each channel TP9 and TP10. The model would then be trained and tested using the recording data to see its possibility of predicting the action.

The signals were showed in Fig. 3. Data shown in Fig. 3 was the recording of EEG signals in around twenty seconds for each individual eye open and close. The recording was started first with open eyes with a total data count of 5712 for 22.3 seconds and then followed by closed eyes with 5412 of data count for about 21.1 seconds.

Channels were indicated as discussed before in Fig. 1. They were TP9, TP10, and some other frontal points AF7, AF8, and Aux for Auxiliary. It could be seen directly from the figures that AF7 and AF8 had an almost similar range of values for both eyes open and close. The only possible way to get the differences between those eye movements came from TP9 and TP10. From both channels, they had different ranges. There were parts which have high values during the close condition. This possibility of different values could be utilized as the detection of features of eye movement.

### 3.3 Prediction of closing eyes

The number of machine learning applications had been increased faster nowadays than before as in epilepsy [40]. It was due to support from many hi-tech companies, such as Google with its Tensorflow [23]. This work had been using that Tensorflow with its Keras application. It utilized the historical data on eye activities. Although statistics had shown the gap difference, it still did not have a clear model to detect an individual activity. To have a definite transfer function from the EEG signals, we desired to use Tensorflow as the machine learning framework. Using the TP9 and TP10 as input, the model would use them as an array of inputs and a prediction of an eye movement as the output. The tread of the learning process is shown in Fig. 4.

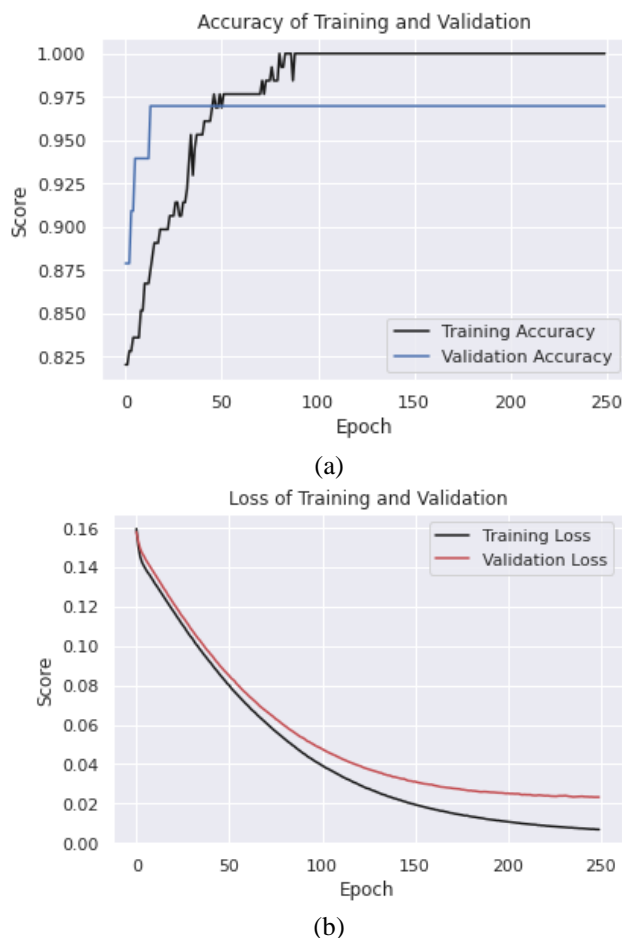


Figure. 4 Detection accuracy and loss: (a) Accuracy and (b) Loss

From Fig. 4, there was an indication that the eye movement was detected using just two basic eye movements: opened and closed conditions. This made an opportunity for epilepsy detection as it was also discussed for children [9]. Further analysis has been made to show the differences which might come from this improvement in this machine learning application. The result of our machine learning process is shown in Fig. 4. We could get more than 96% accuracy and loss only 2.35% from training and test. Fig. 4 (a) shows the accuracy history of the training. The score rose from 0.825 to 1.0 which was similarly from 82.5% to 100%. Next Fig. 4 (b) shows us the loss values in the same process. It was in reverse trend with its accuracy values. It was declining from 16% to a value lower than 2%. Those numbers proved our confidence in using the Muse headband to help epilepsy patients in absence seizures.

To comprehend our machine learning model, it was possible to check its transfer function by using the prediction score as output and two chosen channels, TP9 and TP10 as inputs. The Transfer



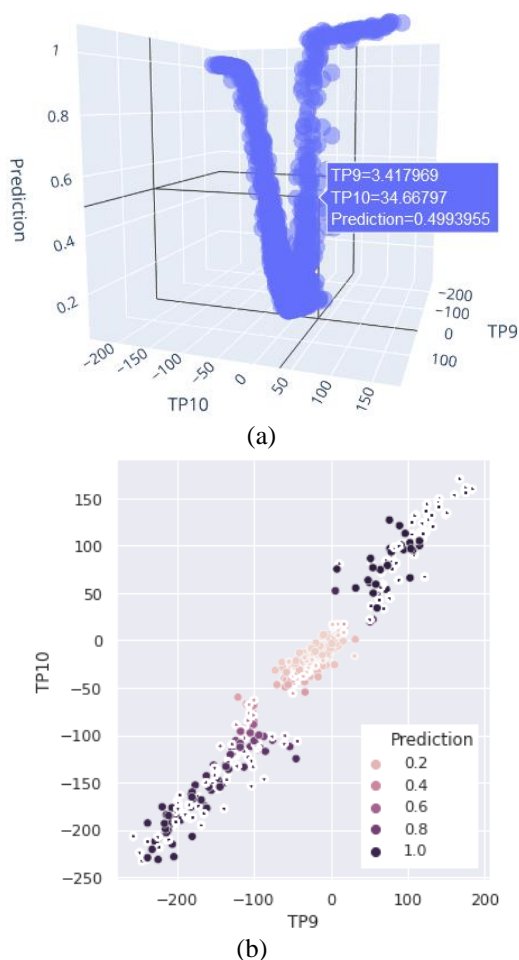


Figure. 5 Prediction: (a) Transfer Function. This is 3D representation of the prediction model. One position which was at TP9=3.42 and TP10=34.67, gives result at 49.93% and (b) Sample data. This is 2D data results. The prediction values are mapped in different colors.

function plot was shown in the 3D form in Fig. 5 (a). The figure has the input plane of TP9 and TP10 as its X and Y coordinates. Then, the prediction of closing eyes was defined at Z-axis as height output. It gave us the one value at values with ranges less than -80uV in TP9 and TP10. However, it is in the slope curve with declining values as the percentage of confidence. It means that the lower value was still having the possibility of closing eyes but less likely to happen. Again, increasing the input values of TP9 and TP10 could lower the value down to 0.2 before going into an uphill curve. Finally, it went back to the value of 1 for values ranging more than 30uV. A 2D map of these values was also provided in Fig. 5 (b).

### 3.4 Measurement divergence

In this part, we would try to see the uniformity of the data obtained between Subject 1, which had been discussed previously, compared to other people.

Table 4. Subject’s profile for measurement’s divergence

Code	Label	Sex	Age	Hair Condition
S1	Subject 1	Male	41	Short
S2	Subject 2	Female	39	Long
S3	Subject 3	Female	38	Short

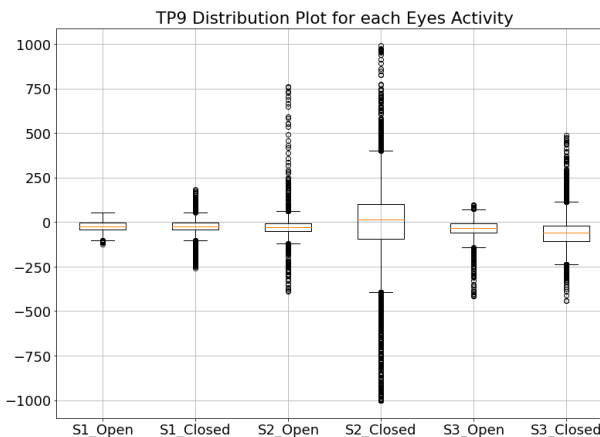


Figure. 6 Distribution plot for eyes activity from TP9 channel

Assuming that if the range of data obtained would be the same, then there was a possibility that the training model could be created only once and just applied to other users without any changes. However, if it was not same, then the training model might need to be trained for each individual subject. Then, it might also support the idea that everyone had their own unique characteristic.

Table 4 showed the subject’s profile that voluntarily helped this research. Following the results of Subject 1, the channels being used were TP9 and TP10. For that reason, next presented data was distribution of data from those two channels to show the possible similarities and differences of each subject.

It could be seen from Fig. 6 obtained from TP9 channel that the open eyes condition had a smaller range of value compared with the closed eyes value. Then, it was also showed that the data obtained followed normal distribution with the median value, which was indicated by the red line, was located in the middle of the box. However, there were differences in the range of values obtained between subjects. Subject 1 had 50% of the data in a smaller range in comparison with subject 2 and 3. It could also be seen in Subject 2 and 3 that the differences in the range of open and closed eyes were greater. Meanwhile, Subject 1 had almost the same gap between those two conditions. The outlier values somehow were still located in a bigger gap in the closed eye compared with open eye activity.

Data from TP9 at Fig. 6 also showed a pattern that

Table 5. Subject’s data homogeneity

Cd.	Ch.	Open			Close		
		Mean	std	%cv	mean	Std	%cv
S1	TP9	-22.73	24.25	-107	-25.54	36.09	-141
	TP10	-19.70	16.99	-86	-23.03	32.54	-141
S2	TP9	-26.74	74.22	-278	-9.91	237.44	-2,397
	TP10	-20.75	66.46	-320	-37.41	237.03	-634
S3	TP9	-36.43	50.71	-139	-58.48	79.59	-136
	TP10	-27.51	33.64	-122	3.35	90.40	2,696

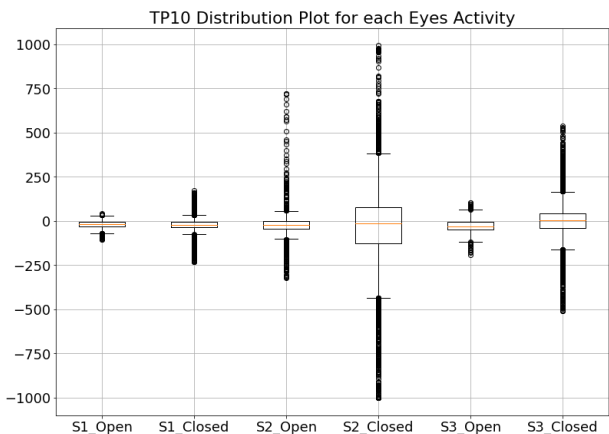


Figure. 7 Distribution plot for eyes activity from TP10 channel

was more or less the same as TP10 at Fig. 7. The difference between the two channels could still be seen although not much. Overall from these two channels, the range of possible values for the closed eye condition was greater than the open eye condition.

The data then could be justified with one more parameter to see its homogeneity. This would quantify the visual approach from the chart described earlier. The parameter was the coefficient of variation (CV). This could be calculated using the known formula in Eq. (15).

$$CV = \frac{\sigma}{\mu} \times 100 \tag{15}$$

Parameter values and CV of each data could be seen in Table 5. It could be seen that the homogeneity of the data obtained for each individual is not the same.

The value of each eye condition was also not same for each individual and channel. This indicates that there is a divergence in the measurements. Most likely the source of the divergence of these measurements was due to the condition from the headband placement itself. It first could understand that the portable headband was using two kinds of electrodes. For surface electrodes, it could be caused by several things from the user’s skin. Some of us might have more sweat on our foreheads while some didn’t. This could affect the surface electrode

measurements which used in AF7, AF8, and AUX sensors at the forehead.

Next, the thickness of subject’s hair around the ear could also affect the conductive sensor electrode which used in TP9 and TP10. It was shown by Table 5 with its increasing CV value especially at closed eyes condition with order of S1, S3, and S2 respectively. As an illustration of the conditions of this headband’s electrode placements, Fig. 8 showed the application of the headband from each subject for comparison with ear-EEG electrodes [19].

### 3.5 Discussion

Recording equipment should be portable and could be used continuously to monitor patients with epilepsy in their daily life. This study is the first to identify the possible use of the Muse headband in detecting absence seizures using channel TP9 and TP10 recordings. In this current work, we assessed the potential for recording EEG and detecting absence seizures from only those two electrodes located around the ear, which is a new method for detection of seizures accidentally like ear-EEG. Future wearable seizure detection systems will use sensors that capture EEG around the ear [19]. If integrated into clinical research with neurologists for treating epilepsy patients, we believe that this study will help them to identify absence seizure using eye activity detection.

Overall, it is shown in Fig. 5 that the detection of closing eyes is possible. By exercising the closed eyes to get confidence level, there was the possibility to detect the absence seizures. That was by having the lowest level of close eyes prediction for a period of time. In this case, its MAD values could be in unique ranges of values as indicated by Fig. 6 and 7. That might be trained for their individual closing and opening eyes. Since the detection rate would vary across individual patients, the ANN would be the best approach for this case [41]. The values would be adjusted through the size and geometry of the patient’s head with an EEG headband.

The contribution of this paper is evidence that the ear sensors on the Muse headband could be used to detect absence seizure in comparison with the general

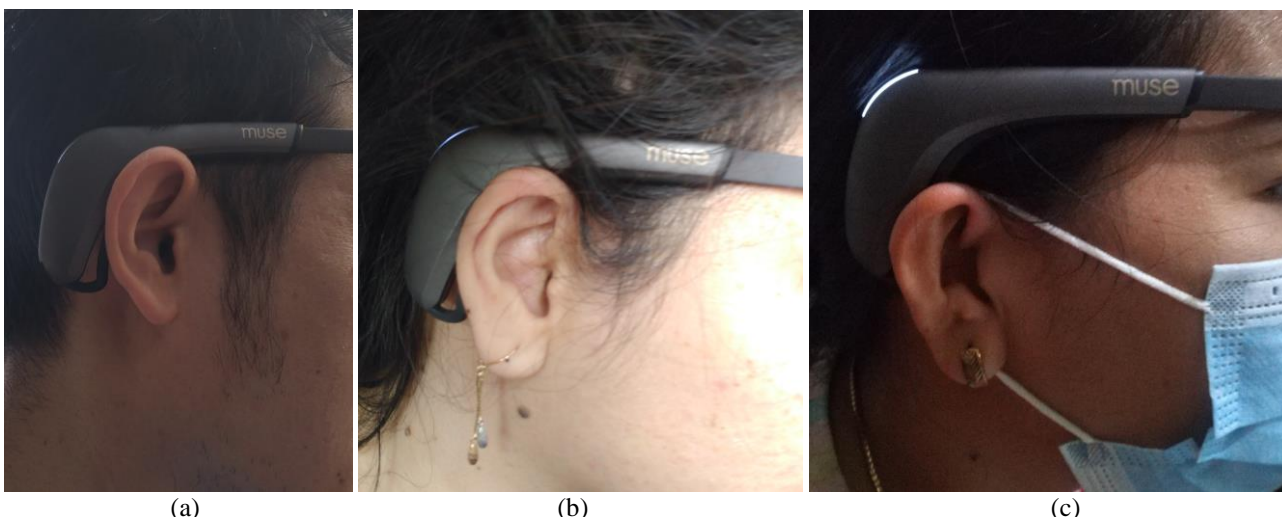


Figure. 8 Ear sensor application of Muse EEG headband Cf. ear-EEG: (a) Subject 1 (S1), (b) Subject 2 (S2) and (c) Subject 3 (S3)

Table 6. Muse headband measurement comparison

Research Target	Field	Method	AF				TP		Aux	Max. Acc.
			7	8	9	10	9	10		
Emotional wellbeing in urban wilderness [15]	Psychology	Statistical	Y	Y	Y	Y	Y	Y	-	
Perceived Mental Stress Classification [42]	Diagnosis	MLP	Y	Y	Y	Y	Y	Y	93%	
Predicting stroke severity [33]	Diagnosis	Random Forest	N	N	Y	Y	N	N	76%	
<b>Closing Eyes Detection</b>	Diagnosis	SVM + MLP	N	N	Y	Y	N	N	96%	

seizures in ear-EEG which have been studied in [19]. Behind-the-ear EEG settings such as ear-EEG may offer more features in treating epilepsy patients. In implementation, the existence of many commercial items already at the market which can be categorized into low-cost, portable EEG systems was a key advantage for overall progress in terms of time [14]. However, a comparison between ear-EEG and commercial EEGs which have been mass-produced cannot be done because of customization, which might not be possible. In fact, comparing items for certain brands can be easily done in terms of use, for example from the EEG channel used, its research method, and how the result’s accuracy is. Comparison of our method with other measurements which also used Muse headband can be seen in Table 6.

From Table 6, it can be seen that the channel used in this method is the same as that used in predicting stroke severity [33], namely, by using the ear Sensor on the TP9 and TP10. However, the maximum accuracy (Max. Acc.) obtained can be 20% better. Then, the results which are almost the same with a difference of 3% can be compared with the perceived mental stress classification [42]. However, the channel used is deeper than our research. All of this research is a development of a common application of the official use of the Muse headband itself which is used generally for meditation tools [43]. This can

be seen from the research on the relationship between emotional and scenery [15].

However, the difference through episodes of seizures should have been taken care of through the ANN training. This could be our next research with known epilepsy patients for a real application which may give a different value for every single person. A number of electrodes that exists did make limitation for epilepsy source detection. A limited number of electrodes constrained the scanning area of the head. To have few motoric movements and other activities could be seen as possible using the available electrodes but to pick up the cause of epilepsy signals might demand a wider area of the head with more electrodes. Overall, it could provide affordable Health System Access, and it might help the patients to know better about their conditions. As to have good health and well-being has been part of understanding ourselves and keeping forward to improve it in long run.

#### 4. Conclusion

In this article, an experimental study is presented with the aim of identifying the appropriate method for using Muse EEG headband to classify closed eyes so that prolonged open eyes can be categorized into the blank stare category. The Muse headband had the possibility to be used for rapid detection using only

TP9 and TP10 electrodes. The values from those two channels showed the difference between the condition of the eyes open and closed. In the performed test, the possibility of closing eye could be detected with 96% accuracy and only 2.35% loss. Looking at this probability, this machine learning model showed the confidence of real application from acquired transfer function as scientific novelty where there was two range of slope to characterize the EEG signals for eyes close and open conditions. In further testing, using two additional subjects, it was found that there was a comparison of the distribution range between open and closed eye conditions. From the CV value which shows homogeneity, it is found that the closed eye condition consistently has a greater value than the open eye condition. It demonstrates the feasibility of detecting absence seizures for epilepsy patients as in ear-EEG system. In the future, the model could be used to develop the cognitive health warning system for communities around the epilepsy patients.

### Conflicts of interest

The authors declare no conflict of interest.

### Author contributions

Erwin Sutanto was typing and managing for this article as the first author and corresponding author. Teguh Wijaya Purwanto was responsible for the chrome plugin software. Fahmi and Wervyan Shalannanda were responsible for the hardware and IoT System. Meanwhile, M. Yazid was assisting in the analysis of machine learning improvement. M. Aziz is taking care of editing and proofreading.

### Acknowledgments

The authors would like to say thanks to the Ministry of Education and Culture, Research, Technology (Kemendikbudristek), Government of Indonesia, who has funded this research with 2021 Program Penelitian Kolaborasi Indonesia (PPKI).

### References

- [1] G. D. Mitsis, M. N. Anastasiadou, M. Christodoulakis, E. S. Papathanasiou, S. S. Papacostas, and A. Hadjipapas, "Functional brain networks of patients with epilepsy exhibit pronounced multiscale periodicities, which correlate with seizure onset", *Human Brain Mapping*, Vol. 41, No. 8, pp. 2059–2076, 2020.
- [2] M. Maschio, A. Zarabla, A. Maialetti, D. Giannarelli, T. Koudriavtseva, V. Villani, and S. Zannino, "Perampanel in brain tumor-related epilepsy: Observational pilot study", *Brain and Behavior*, Vol. 10, No. 6, p. e01612, 2020.
- [3] J. Zelano and G. Westman, "Epilepsy after brain infection in adults: A register-based population-wide study", *Neurology*, Vol. 95, No. 24, pp. e3213–e3220, 2020.
- [4] M. C. Guerrero, J. S. Parada, and H. E. Espitia, "Principal components analysis of eeg signals for epileptic patient identification", *Computation*, Vol. 9, No. 12, p. 133, 2021.
- [5] R. W. Homan, J. Herman, and P. Purdy, "Cerebral location of international 10–20 system electrode placement", *Electroencephalography and Clinical Neurophysiology*, Vol. 66, No. 4, pp. 376–382, 1987.
- [6] G. J. Horng, T. C. Lin, K. C. Lee, K. T. Chen, and C. C. Hsu, "Prediction of prognosis in emergency trauma patients with optimal limit gradient based on grid search optimal parameters", *Wireless Personal Communications*, pp. 1–11, 2021.
- [7] A. Y. Kaplan, A. A. Fingelkurts, A. A. Fingelkurts, S. V. Borisov, and B. S. Darkhovsky, "Nonstationary nature of the brain activity as revealed by eeg/meg: methodological, practical and conceptual challenges", *Signal Processing*, Vol. 85, No. 11, pp. 2190–2212, 2005.
- [8] A. Firmansah, A. R. Taufani, I. K. Kusumaningrum, S. N. Maharani, and G. J. Horng, et al., "Iot based less-contact system on sauce production for small enterprises", *Journal of Applied Science and Engineering*, Vol. 25, No. 1, pp. 85–93, 2021.
- [9] M. B. Hunter and R. F. Chin, "Impaired social attention detected through eye movements in children with early-onset epilepsy", *Epilepsia*, Vol. 62, no. 8, pp. 1921–1930, 2021.
- [10] D. Angeles et al., "Proposal for revised clinical and electroencephalographic classification of epileptic seizures", *Epilepsia*, Vol. 22, No. 4, pp. 489–501, 1981.
- [11] M. Yazid, F. Fahmi, E. Sutanto, W. Shalannanda, R. Shoalihin, and G. J. Horng, et al., "Simple detection of epilepsy from eeg signal using local binary pattern transition histogram", *IEEE Access*, Vol. 9, pp. 150252 – 150267, 2021.
- [12] G. Lantz, R. G. D. Peralta, L. Spinelli, M. Seeck, and C. Michel, "Epileptic source localization with high density eeg: how many electrodes are needed?", *Clinical*

- Neurophysiology*, Vol. 114, No. 1, pp. 63–69, 2003.
- [13] A. Shoeb, H. Edwards, J. Connolly, B. Bourgeois, S. T. Treves, and J. Gutttag, “Patient-specific seizure onset detection”, *Epilepsy & Behavior*, Vol. 5, No. 4, pp. 483–498, 2004.
- [14] O. E. Krigolson, C. C. Williams, A. Norton, C. D. Hassall, and F. L. Colino, “Choosing muse: Validation of a low-cost, portable eeg system for erp research”, *Frontiers in Neuroscience*, Vol. 11, p. 109, 2017.
- [15] K. Herman, L. Ciechanowski, and A. Przegalin’ska, “Emotional wellbeing in urban wilderness: Assessing states of calmness and alertness in informal green spaces (igss) with muse—portable eeg headband”, *Sustainability*, Vol. 13, No. 4, p. 2212, 2021.
- [16] A. Asif, M. Majid, and S. M. Anwar, “Human stress classification using eeg signals in response to music tracks”, *Computers in Biology and Medicine*, Vol. 107, pp. 182–196, 2019.
- [17] F. Brigo, E. Trinka, S. Lattanzi, N. L. Bragazzi, R. Nardone, and M. Martini, “A brief history of typical absence seizures—petit mal revisited”, *Epilepsy & Behavior*, Vol. 80, pp. 346–353, 2018.
- [18] S. D. Jørgensen, I. C. Zibrandtsen, and T. W. Kjaer, “Ear-eeg-based sleep scoring in epilepsy: A comparison with scalp-eeg”, *Journal of Sleep Research*, Vol. 29, No. 6, p. e12921, 2020.
- [19] Y. Gu, E. Cleeren, J. Dan, K. Claes, W. Van Paesschen, S. Van Huffel, and B. Hunyadi, “Comparison between scalp eeg and behind-the-ear eeg for development of a wearable seizure detection system for patients with focal epilepsy”, *Sensors*, Vol. 18, No. 1, p. 29, 2017.
- [20] J. R. Tenney and T. A. Glauser, “The current state of absence epilepsy: Can we have your attention?: The current state of absence epilepsy”, *Epilepsy Currents*, Vol. 13, No. 3, pp. 135–140, 2013.
- [21] M. Bedeuzzaman, T. Fathima, Y. U. Khan, and O. Farooq, “Seizure prediction using statistical dispersion measures of intracranial eeg”, *Biomedical Signal Processing and Control*, Vol. 10, pp. 338–341, 2014.
- [22] A. Subasi and E. Ercelebi, “Classification of eeg signals using neural network and logistic regression”, *Computer Methods and Programs in Biomedicine*, Vol. 78, No. 2, pp. 87–99, 2005.
- [23] A. G’eron, *Hands-on machine learning with Scikit-Learn, Keras, and TensorFlow: Concepts, tools, and techniques to build intelligent systems*, O’Reilly Media, 2019.
- [24] M. Abadi, P. Barham, J. Chen, Z. Chen, A. Davis, J. Dean, M. Devin, S. Ghemawat, G. Irving, and M. Isard, et al., “Tensorflow: A system for large-scale machine learning”, In: *Proc. of 12th USENIX Symposium on Operating Systems Design and Implementation*, pp. 265–283, 2016.
- [25] R. S. Fisher, J. H. Cross, J. A. French, N. Higurashi, E. Hirsch, F. E. Jansen, L. Lagae, S. L. Mosh’e, J. Peltola, and E. R. Perez, et al., “Operational classification of seizure types by the international league against epilepsy: Position paper of the ilae commission for classification and terminology”, *Epilepsia*, Vol. 58, No. 4, pp. 522–530, 2017.
- [26] M. A. Kramer, U. T. Eden, K. Q. Lepage, E. D. Kolaczyk, M. T. Bianchi, and S. S. Cash, “Emergence of persistent networks in long-term intracranial eeg recordings”, *Journal of Neuroscience*, Vol. 31, No. 44, pp. 15757–15767, 2011.
- [27] R. Livingston, “The cerebral cortex and consciousness”, *Clinical Neurosurgery*, Vol. 3, pp. 192–202, 1955.
- [28] H. Jasper, “Wilder penfield: his legacy to neurology. the centrencephalic system.”, *Canadian Medical Association Journal*, Vol. 116, No. 12, p. 1371, 1977.
- [29] M. Mart’inez, S. Masakazu, C. Munari, R. Porter, J. Roger, and P. Wolf, et al., “Commission on classification and terminology of the international league against epilepsy. proposal for revised classification of epilepsies and epileptic syndromes”, *Epilepsia*, Vol. 30, No. 4, pp. 389–99, 1989.
- [30] H. Lu’ders, J. Acharya, C. Baumgartner, S. Benbadis, A. Bleasel, R. Burgess, D. Dinner, A. Ebner, N. Foldvary, and E. Geller, et al., “Semiological seizure classification.”, *Epilepsia*, Vol. 39, No. 9, pp. 1006–1013, 1998.
- [31] A. C. N. Society et al., “Guideline 5: guidelines for standard electrode position nomenclature”, *American Journal of Electroneurodiagnostic Technology*, Vol. 46, No. 3, pp. 222–225, 2006.
- [32] O. Valentin, G. Viallet, A. Delnavaz, G. C. Richert, M. Ducharme, H. M. Chanon, and J. Voix, “Custom-fitted in-and around-the-ear sensors for unobtrusive and on-the-go eeg acquisitions: development and validation”, *Sensors*, Vol. 21, No. 9, p. 2953, 2021.

- [33] C. M. Wilkinson, J. I. Burrell, J. W. Kuziek, S. Thirunavukkarasu, B. H. Buck, and K. E. Mathewson, "Predicting stroke severity with a 3-min recording from the muse portable eeg system for rapid diagnosis of stroke", *Scientific Reports*, Vol. 10, No. 1, pp. 1–11, 2020.
- [34] U. Shaked, "eeg-explorer", <https://github.com/urish/eeg-explorer>, 2018.
- [35] S. Xie, "Wavelet power spectral domain functional principal component analysis for feature extraction of epileptic eegs", *Computation*, Vol. 9, No. 7, p. 78, 2021.
- [36] U. Shaked, "muse-js." <https://github.com/urish/muse-js>, 2020.
- [37] jquery, "jquery." <https://jquery.com/>, 2020.
- [38] popper, "popper." <https://popper.js.org/>, 2021.
- [39] E. Sutanto, F. Fahmi, W. Shalannanda, and A. Aridarma, "Cry recognition for infant incubator monitoring system based on internet of things using machine learning", *International Journal of Intelligent Engineering and Systems*, Vol. 14, No. 1, pp. 444–454, 2021, doi: 10.22266/ijies2021.0228.41.
- [40] A. H. Shoeb, "Application of machine learning to epileptic seizure onset detection and treatment. PhD thesis", *Massachusetts Institute of Technology*, 2009.
- [41] U. R. Acharya, S. L. Oh, Y. Hagiwara, J. H. Tan, and H. Adeli, "Deep convolutional neural network for the automated detection and diagnosis of seizure using eeg signals", *Computers in Biology and Medicine*, Vol. 100, pp. 270–278, 2018.
- [42] A. Arsalan, M. Majid, A. R. Butt, and S. M. Anwar, "Classification of perceived mental stress using a commercially available eeg headband", *IEEE Journal of Biomedical and Health Informatics*, Vol. 23, No. 6, pp. 2257–2264, 2019.
- [43] I. InteraXon, "Muse™ eeg powered meditation and sleep headband.", <https://choosemuse.com/>, 2021.